

# Comparison of Collection Efficiency of ESP in a Numerical Model Using One and Multiple Independent Power Supplies

László Székely<sup>1\*</sup>, István Kiss<sup>1</sup>

<sup>1</sup> Department of Electric Power Engineering, Faculty of Electrical Engineering and Informatics, Budapest University of Technology and Economics, Műgyetem rkp. 3., H-1111 Budapest, Hungary

\* Corresponding author, e-mail: [szekely.laszlo@vet.bme.hu](mailto:szekely.laszlo@vet.bme.hu)

Received: 27 April 2023, Accepted: 05 June 2023, Published online: 22 August 2023

## Abstract

This work modeling the collection efficiency of an ESP numerical model based on industrial plant development. Under high dust loads, one power supply controlled the voltages on the two separation zones. The separation efficiency is different depending on the diameter of the dust particles, so the two zones receive dust particles with various distributions, and the electrical characteristics are not the same. In this article, we show the change in the efficiency of separation when the two zones are controlled at different voltages by power supplies.

## Keywords

electrostatic precipitator, numerical model, separation efficiency, dust

## 1 Introduction

Air pollution is becoming a significant problem in more and more places worldwide, as rapid economic development has drastically increased pollutant emissions [1, 2]. Power plants and large industrial plants with high environmental impact are now unthinkable without some technology to keep emissions below limits [3, 4]. Although fewer coal-fired power plants are being built as renewables and other clean energy sources become more widespread, emerging issues make it critical to limit the amount of air pollution (e.g., increased urban pollution) [5].

Electrostatic precipitators (ESPs) are used in many parts of the world, helping to protect our environment from high dust loads. In addition to relatively high installation costs, it has several advantages, including a collection efficiency of almost 100%, the ability to perform well under high dust loads, and a wide operating temperature range [6, 7]. However, it is essential to note that an ESP can only perform well with the proper settings. Active research is being carried out into different electrode arrangements or changes in supply voltage, temperature or e.g., air velocity differences [6–10].

For multi-zone ESP-s, it is essential to consider the characteristics of the dust entering the zones. Generally, larger particles in a dust stream will be collected by the incoming air in the first part of the zone. The collection is facilitated

by the turbulent flow and the fact that the charged particles when they get close to the collecting electrode, move toward the ground electrode under the influence of electrostatic forces. The challenge is more significant for small (0.5–2  $\mu\text{m}$ ) particles because, given a unit mass of dust (or dust particles), they can accumulate more charge in specific due to their larger specific surface area, thus forming a dust space charge region. It is noted here that the collection efficiency of particles in the nm range can be increased by implementing AC corona or dielectric-barrier discharge [11]. The charging mechanism is different, with diffusion charging instead of electric field charging; thus, some nanometers to 100  $\mu\text{m}$  particles are not usually separated simultaneously with high efficiency [12, 13].

The effect of space charge is to reduce the intensity of the corona discharges [14], so the number of electrons charging the particles is less, forming charged and uncharged dust blocks. At the same time, the breakdown voltage also varies from case to case since the occurrence of the breakdown voltage is highly dependent on the intensity of the initial partial discharges. In the case of multi-zone ESPs, the two phenomena are present simultaneously, which makes this a significant challenge.

A typical design is to have a single power supply for a single piece of equipment (also an actual situation where

multistage ESPs are built to collect the different dust particles). The main disadvantage of a single power supply solution is that the zone with the lower breakdown voltage will always limit the zone with the higher breakdown voltage. In other words, the second zone is inefficient.

When setting up new equipment, reasonable solutions can still be found by designing the geometry dimensions, but there are few better effective methods for upgrading existing equipment. Improvements in collection efficiency can also be achieved by using pre-filters, pre-chargers, steam recirculation, or by varying the pressure or temperature, but in these cases, it is necessary to modify the technology itself [15–17].

Our article and investigations were motivated by the challenges of refurbishing an existing ESP in an industrial plant where a single power supply supplied two zones. In the processed paper, a 3 m long dust collector with a street layout was simulated; the dust particle charging process and collection efficiency were investigated for one and two independent voltage feeds.

## 2 Numerical model

### 2.1 Model structure

The street layout of the ESP, the electric field, and the flow field are symmetrical in relation to the plane containing the corona electrodes parallel to the flow and located on the center line of the streets. Assume a single half-street layout in the model, which several authors use as a simplification [18, 19]. In this case, the symmetry allows the computation to be extended to an entire street and then to approximately the entire ESP while reducing the required computational power to a fraction. The model is designed according to a modular system, consisting of two main modules that apply the donor cell method. The first calculates the electric field based on the supply voltage and the space charge (Eqs. (1)–(7)), while the second calculates the flow field (Eqs. (8) and (9)) and the trajectory of the particles:

$$\begin{aligned} \varphi(P) = & \frac{1}{4\pi\epsilon} \int_V \frac{\rho_V}{r} dV + \frac{1}{4\pi\epsilon} \int_{A_1} \frac{\rho_A}{r} dA \\ & + \frac{1}{4\pi\epsilon} \int_{A_2} \frac{v}{r} \text{grad} \frac{1}{r} dA, \end{aligned} \quad (1)$$

where the first term in the equation represents the effect of the space charge, the second term describes the effect of the surface charges on the surface  $A_1$ , the third term describes the value of the potential from dipole moment  $v$  on the surface  $A_2$ .  $\rho_V$  represents the sum of the ion and

particle charge densities,  $\rho_A$  the surface charge at the corona and collecting electrode, the third part of Eq. (1) can be negligible in the case of ESPs:

$$E = -\text{grad}\varphi, \quad (2)$$

$$\sigma = \mu_i \times \rho_{ion}, \quad (3)$$

$$J = \sigma \times E, \quad (4)$$

$$\text{div}J = 0, \quad (5)$$

$$\text{div}D = \rho_{ion} + \rho_{dust}, \quad (6)$$

$$D = \epsilon E, \quad (7)$$

where  $E$  is the electric field,  $\varphi$  is the potential,  $\rho_{ion}$  and  $\rho_{dust}$  are the ion and dust space charge,  $\mu_i$  is the ion mobility,  $J$  is the ionic current,  $D$  is the displacement,  $\epsilon$  is the relative permittivity of dust particles.

$$v_x \frac{\partial c}{\partial x} + v_y \frac{\partial c}{\partial y} = \frac{\partial}{\partial y} \left( \frac{v_t}{Sc_t} \frac{\partial c}{\partial y} \right) - \frac{\partial}{\partial y} (c \times With_y) \quad (8)$$

$$With_y = \frac{Q_p^\infty E_y}{3\pi\mu d_p} Cu \quad (9)$$

In Eqs. (8) and (9)  $v_x$  and  $v_y$  are the velocity components of the gas flow,  $v_t$  is the kinematic viscosity,  $Sc_t$  is the turbulent Schmidt number,  $With_y$  is the theoretical drift velocity,  $c$  is the dust concentration,  $\mu$  is the dynamic viscosity,  $Cu$  is the Cunningham correction factor,  $Q_p$  and  $d_p$  is the saturation charge and diameter of a spherical particle. Further information can be found in the literature [20]. The final output of the model determines the electric field distribution, the flow velocity distribution, the corona currents (corona discharge intensity), and the total dust and fractions concentration.

### 2.2 Point-plate arrangement and cylindrical symmetry

The symmetry can distinguish two cases within a half street of ESP. Laboratory measurements and industrial installations usually use point-plate arrangement. In terms of the potential distribution created by point-plate arrangement in the numerical model is adequate, but the calculation of the corona currents is worth considering.

The theory behind the phenomenon is that the high-voltage electrode is surrounded by a corona region of a given radius in which the number of charge carriers increases. Leaving the range, the electrons slow down and drift along the electric field strengths towards the collecting electrode.

In model calculations, Peek's law is commonly used, i.e., the critical field strength required to initiate a discharge is determined, which assumes a smooth, cylindrical electrical field. The grounded electrodes had a cylinder of radius  $R_w$ , then the supply voltage  $U_{cr}$  (critical as corona onset voltage) required to create the corona discharge could be expressed as in Eq. (13). Using  $U_{cr}$ , the current  $I$  flowing out of the unit length of the corona electrode under voltage  $U > U_{cr}$  can be calculated. However, in a street arrangement, the  $E$  field is not cylindrical, so instead of the radius (distance) of the grounded electrode, a modified equivalent radius is used, the value of which depends on the ratio of the width to the length of the half-street; by Moore is used [21, 22]. Thus, in effect, the calculation of the corona current is more accurate.

In addition, the voltage-current characteristic should be transposed to the electric field – current density characteristic, using Eqs. (10)–(14):

$$I = J_w \times A, \quad (10)$$

$$A = 2 \times \pi \times R_w \times l, \quad (11)$$

$$J_w = K \times E \times (E - E_{cr}), \quad (12)$$

$$E_{cr} = \frac{U_{cr}}{R_w \times \ln\left(\frac{R_p}{R_w}\right)}, \quad (13)$$

$$R_w = \frac{4 \times W}{2 \times \pi}, \quad (14)$$

where  $I$  is the current,  $J_w$  is the current density,  $A$  is the surface,  $l$  is the length of the corona electrode,  $E$  is the electric field strength,  $E_{cr}$  is the critical (initiating a discharge) electric field strength,  $R_p$  is the radius of corona electrode,  $R_w$  the equivalent outer radius in cylindrical geometry and  $W$  is the width of half street in the point-plate arrangement. The values of  $E_{cr}$  and  $K$  was given from an approximation of measured characteristics.

### 2.3 Comparison of collection efficiency using one and two independent power supplies

In the model, the following parameter were set:

- 0.00155 [m]: radius of corona electrode;
- 3 [m]: street length of the model;
- 0.15 [m]: height of the street in the model;
- 9: number of corona electrode;
- 30 [cm]: distance between two corona electrodes;
- 1 [m/s]: inlet gas speed;

- 100000 [Pa]: pressure of gas;
- 25 [°C]: temperature;
- 0.000218 [m<sup>2</sup>/Vs]: ion mobility;
- 1500 [kg/m<sup>3</sup>]: specific dust mass density;
- 2: relative permittivity;
- 10 [μm]: diameter of dust fraction '1';
- 10 [mg/m<sup>3</sup>]: mass density of fraction '1';
- 5 [μm]: diameter of dust fraction '2';
- 1 [mg/m<sup>3</sup>]: mass density of fraction '2'.

Each simulation had computed with two dust fractions, a larger (10 μm) and a smaller (5 μm) one. The ion mobility was set based on the values used in calculations from the literature [23, 24].

#### 2.3.1 ESP model using one power supply

The single supply voltage examination of the model describes the industrial case where the same power supply controls two zones of the separation chamber. For the model, the maximum supply voltage was 45 kV. The process of dust collection can be observed in Fig. 1.

Fig. 1 shows the rows from top to bottom:

- Potential distribution in a half-street arrangement;
- Flow-field distribution;
- Dust mass density in summarization;
- Dust mass density with fraction '1' (considering only 10 μm particles);
- Dust mass density with fraction '2';

At half of all coronal electrode distances a region with low electric field are present, so an empty band is observed at the boundary, representing the transition band under boundary conditions.

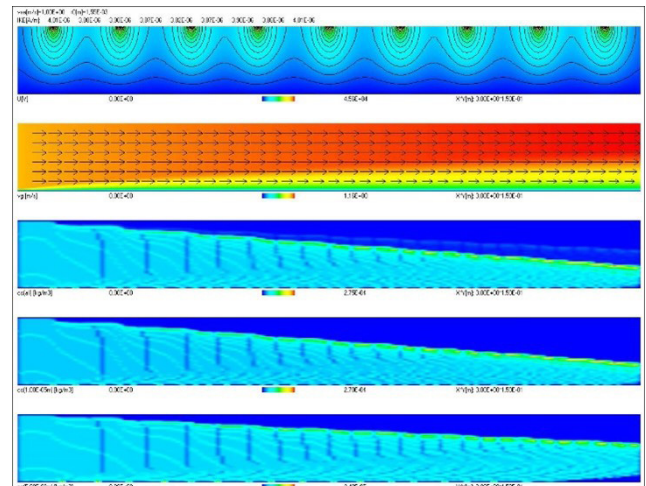


Fig. 1 Separation processes using one power supply

From the rows of Fig. 1, it can be roughly traced that most (not all) of the 10-micron particles precipitate, while a significant proportion of the 5-micron particles do not. Of course, the third row in Fig. 1, which presents the dust mass density in summarization, shows a distortion, as most of the total amount of dust will be in the 10-micron range, so the color scale is less likely to show significant exudation of the 5-micron particles due to the relative proportions. (In the figure it can also be observed some words in small letters; the info there can be found in parameter settings in Section 2.3.)

### 2.3.2 ESP model using two independent power supplies

The two-power supply case represents a real-life situation where several zones of a dust collection chamber are separately controlled. In this case, the zone with the higher breakdown voltage will not be limited by the maximum allowable voltage of the zone from the lower side.

Since the distribution of field strength and dust charge also varies due to the different dust compositions, the model created in this way is more accurate than previous models [25–27].

The parameter set-up of the new case in the model is the same as the previous one, expect the change of corona electrodes' operational voltage. The corona electrode voltage is 45 kV for the first five and 63 kV for the last four. The result can be seen in Fig. 2.

Fig. 2 shows a higher density of potential lines in the second half of the zone, resulting in a more intense separation. A change in the curve of the deposition process can be observed in rows 3–5, as the slope has become steeper. Some of the dust particles have now also reached the end of the street (in real cases, exhaust chimney), but to a lesser extent.

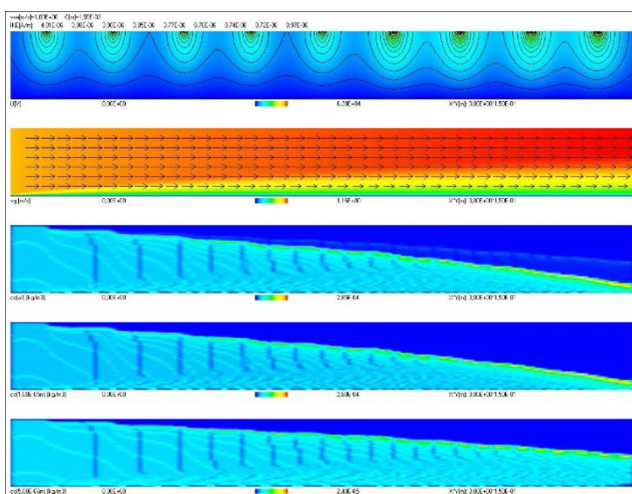


Fig. 2 Separation processes using two power supplies

### 2.3.3 Differences in efficiency

The model saves the actual efficiency of collection at each distance point every 4.3 cm along the 'x' axis, calculated from the ratio of the incoming dust volume to the proportion of dust particles reaching the 'y' = 0 boundary plane. The efficiency of the single and dual feed examination is shown in Figs. 3 and 4.

The saved values of the model show that the collection efficiency reaches 80% in the one-power case, which is a low value for ESPs. For smaller fractions the collection efficiency is 50%. The SUM value is shifted to around 80% due to the higher mass of the 10-micron particles, but it should be remembered that the range of particles that are harmful to health mainly includes particles of a few microns and below.

In the case of two feeds, the separation improves to almost 90%, with smaller particles separating at 57%. The flattening of the curves is due to the saturation of the dust particles and the appearance of dust space charge. Since there is a transition band at the interfaces, the modeled ESP can produce a few % improvements compared to

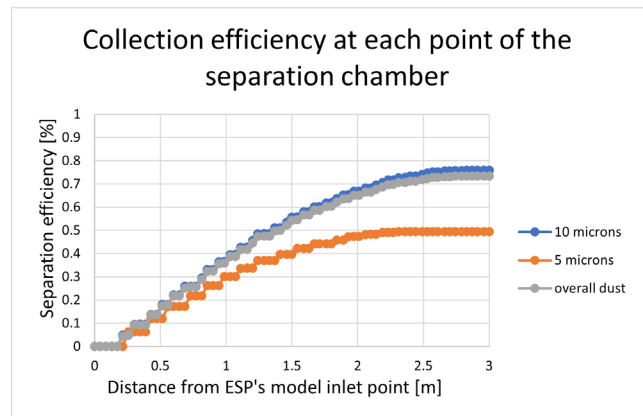


Fig. 3 Efficiency of collection per unit saved in the numerical model – using one power supply

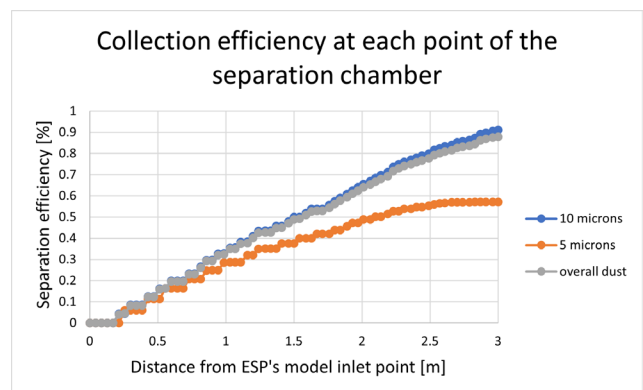


Fig. 4 Efficiency of collection per unit saved in the numerical model – using two power supplies

the real case. The exact separation efficiency in these two cases can be seen in Table 1.

Separate zone control has improved the efficiency of particle collection for all fractions. Collection efficiency improved by 15.1% for larger particles, 7.4% for smaller particles and 14.4% for total dust.

**Table 1** Collection efficiency of dust's fraction in different supply modes

Supply mode	Sep.Eff. SUM [%]	Sep.Eff. 10 $\mu\text{m}$ [%]	Sep.Eff. 5 $\mu\text{m}$ [%]
1	73.5	75.9	49.5
2	87.9	91.0	57.1

## References

- [1] Zheng, S., Kahn, M. E. "Understanding China's urban pollution dynamics", *Journal of Economic Literature*, 51(3), pp. 731–772, 2013.  
<https://doi.org/10.1257/jel.51.3.731>
- [2] Newman, J. D., Bhatt, D. L., Rajagopalan, S., Balmes, J. R., Brauer, M., Breyse, P. N., Brown, A. G. M., Carnethon, M. R., Cascio, W. E., Collman, G. W., Fine, L. J., ..., Brook, R. D. "Cardiopulmonary impact of particulate air pollution in high-risk populations: JACC state-of-the-art review", *Journal of the American College of Cardiology*, 76(24), pp. 2878–2894, 2020.  
<https://doi.org/10.1016/j.jacc.2020.10.020>
- [3] Shi, W., Lin, C., Chen, W., Hong, J., Chang, J., Dong, Y., Zhang, Y. "Environmental effect of current desulfurization technology on fly dust emission in China", *Renewable and Sustainable Energy Reviews*, 72, pp. 1–9, 2017.  
<https://doi.org/10.1016/j.rser.2017.01.033>
- [4] Xi, J. F., Gu, Z. Z., Cai, J., Zhang, J., Wang, H. C., Wang, S. F. "Filtration of dust in an electrostatically enhanced granular bed filter for high temperature gas cleanup", *Powder Technology*, 368, pp. 105–111, 2020.  
<https://doi.org/10.1016/j.powtec.2020.03.070>
- [5] von Schneidmesser, E., Steinmar, K., Weatherhead, E. C., Gerwig, H., Quedenau, J. "Air pollution at human scales in an urban environment: Impact of local environment and vehicles on particle number concentrations", *Science of the Total Environment*, 688, pp. 691–700, 2019.  
<https://doi.org/10.1016/j.scitotenv.2019.06.309>
- [6] Xu, X., Gao, X., Yan, P., Zhu, W., Zheng, C., Wang, Y., Luo, Z., Cen, K. "Particle migration and collection in a high-temperature electrostatic precipitator", *Separation and Purification Technology*, 143, pp. 184–191, 2015.  
<https://doi.org/10.1016/j.seppur.2015.01.016>
- [7] Mizuno, A. "Electrostatic precipitation", *IEEE Transactions on Dielectrics and Electrical Insulation*, 7(5), pp. 615–624, 2000.  
<https://doi.org/10.1109/94.879357>
- [8] Fayyad, M. B., González, A. A., Iváncsy, T. "Numerical study of the influence of using crenelated collecting plates on the electrostatic precipitators", *Journal of Electrostatics*, 123, 103811, 2023.  
<https://doi.org/10.1016/j.elstat.2023.103811>
- [9] Fayyad, M. B., González, A. G. A., Iváncsy, T. "The effects of the corona wire distribution with triangular collecting plates on the characteristics of electrostatic precipitators", In: 2022 International Conference on Diagnostics in Electrical Engineering (Diagnostika), Pilsen, Czech Republic, 2022, pp. 1–7. ISBN 978-1-6654-8083-3  
<https://doi.org/10.1109/Diagnostika55131.2022.9905103>
- [10] Bidoggia, B., Larsen, M. K., Poulsen, K., Skriver, K. "Reduction of dust emission by Coromax micro-pulse power supplies at an oil shale fired power plant", *Journal of Electrostatics*, 105, 103447, 2020.  
<https://doi.org/10.1016/j.elstat.2020.103447>
- [11] Kim, J.-H., Lee, H.-S., Kim, H.-H., Ogata, A. "Electrospray with electrostatic precipitator enhances fine particles collection efficiency", *Journal of Electrostatics*, 68(4), pp. 305–310, 2010.  
<https://doi.org/10.1016/j.elstat.2010.03.002>
- [12] Li, M., Christofides, P. D. "Collection efficiency of nanosize particles in a two-stage electrostatic precipitator", *Industrial & Engineering Chemistry Research*, 45(25), pp. 8484–8491, 2006.  
<https://doi.org/10.1021/ie060101r>
- [13] Lin, G.-Y., Tsai, C.-J., Chen, S.-C., Chen, T.-M., Li, S.-N. "An efficient single-stage wet electrostatic precipitator for fine and nano-sized particle control", *Aerosol Science and Technology*, 44(1), pp. 38–45, 2010.  
<https://doi.org/10.1080/02786820903338298>
- [14] Zheng, C., Zhang, X., Yang, Z., Liang, C., Guo, Y., Wang, Y., Gao, X. "Numerical simulation of corona discharge and particle transport behavior with the particle space charge effect", *Journal of Aerosol Science*, 118, pp. 22–33, 2018.  
<https://doi.org/10.1016/j.jaerosci.2018.01.008>
- [15] Jaworek, A., Marchewicz, A., Sobczyk, A. T., Krupa, A., Czech, T. "Two-stage electrostatic precipitators for the reduction of PM2.5 particle emission", *Progress in Energy and Combustion Science*, 67, pp. 206–233, 2018.  
<https://doi.org/10.1016/j.peccs.2018.03.003>
- [16] Day, D. B., Xiang, J., Mo, J., Clyde, M. A., Weschler, C. J., Li, F., Gong, J., Chung, M., Zhang, Y., Zhang, J. "Combined use of an electrostatic precipitator and a high-efficiency particulate air filter in building ventilation systems: Effects on cardiorespiratory health indicators in healthy adults", *Indoor Air*, 28(3), pp. 360–372, 2018.  
<https://doi.org/10.1111/ina.12447>

## 3 Conclusion

This paper presented a numerical simulation examination of collection efficiency in the case of using one and double independent voltage supplies. Considering the dust properties difference between each zone, the electric field distribution, charge and collection processes differ. For the same incoming dust volume and geometric parameters of ESP, the collection efficiency in the separately fed zones improved by 15% for larger particles and 8% for smaller particles. Due to the increased voltage of the corona electrodes in the second zone, the discharge intensity is more active, dust particles are continuously charged and thus the precipitation around the collecting electrode is faster.

- [17] Luo, K., Li, Y., Zheng, C., Gao, X., Fan, J. "Numerical simulation of temperature effect on particles behavior via electrostatic precipitators", *Applied Thermal Engineering*, 88, pp. 127–139, 2015.  
<https://doi.org/10.1016/j.applthermaleng.2014.11.078>
- [18] Zhu, Y., Gao, M., Chen, M., Shi, J., Shangguan, W. "Numerical simulation of capture process of fine particles in electrostatic precipitators under consideration of electrohydrodynamics flow", *Powder Technology*, 354, pp. 653–675, 2019.  
<https://doi.org/10.1016/j.powtec.2019.06.038>
- [19] Anagnostopoulos, J., Bergeles, G. "Corona discharge simulation in wire-duct electrostatic precipitator", *Journal of Electrostatics*, 54(2), pp. 129–147, 2002.  
[https://doi.org/10.1016/S0304-3886\(01\)00172-3](https://doi.org/10.1016/S0304-3886(01)00172-3)
- [20] Iváncsy, T., Kiss, I., Berta, I. "Improved model for the analysis of back corona in pulse energised electrostatic precipitators", *Journal of Electrostatics*, 67(2–3), pp. 146–149, 2009.  
<https://doi.org/10.1016/j.elstat.2009.01.057>
- [21] Moore, A. D. "Electrostatics and its applications", Wiley, New York, NY, USA, 1973.
- [22] Brocilo, D., Chang, J. S., Findlay, R. D., Kawada, Y., Ito, T. "Modelling of the effect of electrode geometries on the corona discharge current-voltage characteristic for wire-plate electrostatic precipitators", In: 2001 Annual Report Conference on Electrical Insulation and Dielectric Phenomena (Cat. No.01CH37225), Kitchener, ON, Canada, 2001, pp. 681–684. ISBN 0-7803-7053-8  
<https://doi.org/10.1109/CEIDP.2001.963637>
- [23] Elmoursi, A. A., Castle, G. S. P. "Modeling of corona characteristics in a wire-duct precipitator using the charge simulation technique", *IEEE Transactions on Industry Applications*, IA-23(1), pp. 95–102, 1987.  
<https://doi.org/10.1109/TIA.1987.4504872>
- [24] Sayed, A. M., Abouelatta, M. A., Badawi, M., Mahmoud, K., Lehtonen, M., Darwish, M. M. F. "Novel accurate modeling of dust loaded wire-duct precipitators using FDM-FMG method on one fine computational domains", *Electric Power Systems Research*, 203, 107634, 2022.  
<https://doi.org/10.1016/j.epsr.2021.107634>
- [25] Kiss, I., Suda, J. M., Kristóf, G., Berta, I. "The turbulent transport process of charged dust particles in electrostatic precipitators", In: 7th International Conference on Electrostatic Precipitation, Kyongju, Korea, 1998, pp. 196–205.
- [26] Iváncsy, T., Kiss, I., Berta, I. "Numerical analysis of the effect of pulse energisation on back corona formation in electrostatic precipitators", In: Proceedings of 15th International Symposium on High Voltage Engineering, Ljubljana, Slovenia, 2007, T1–740.
- [27] Iváncsy, T., Suda, J. M., Kiss, I., Berta, I. "Novel ESP model for impulse energisation", In: Proceedings of the X. International Conference on Electrostatic Precipitation, Cairns, Australia, 2006, 6B3.